



ELSEVIER

**Inorganica
Chimica Acta**

Inorganica Chimica Acta 228 (1995) 219–224

Metal cluster topology

17. Hypervalent indium vertices in isolated hypoelectronic indium polyhedra in binary and ternary intermetallic phases of indium and alkali metals [☆]

R.B. King

Department of Chemistry, University of Georgia, Athens, GA 30602, USA

Received 13 May 1994; revised 5 September 1994

Abstract

Analyses of the structures and electron counts for the known isolated indium clusters found in binary and ternary alkali-metal–indium intermetallic phases using methods derived from graph theory suggest the presence of hypervalent indium vertices using filled indium d orbitals as well as sp^3 orbitals for skeletal bonding to relieve the apparent electron poverty in the hypoelectronic polyhedra. The novel shapes of the hypoelectronic indium polyhedra in such clusters are based on capping a triangular or rectangular face of a smaller polyhedron, followed by flattening the pyramid generated by the capping vertex so that it moves closer to the center of the polyhedron. Reasonable electron counts and globally delocalized bonding topologies are then obtained for the hypoelectronic indium clusters if all of the indium vertices at the flattened polyhedral sites are hypervalent using sp^3d five-orbital manifolds and the remaining indium vertices are normal using sp^3 four-orbital manifolds, like typical vertex atoms in boranes, carboranes and post-transition metal ‘Zintl-type’ clusters. For example, the empty triflattened pentacapped trigonal prismatic indium cluster anion In_{11}^{7-} in K_8In_{11} and $K_8In_{10}Hg$ becomes a globally delocalized 11-vertex deltahedron with three hypervalent and eight normal indium vertices and the required $2n + 2 = 24$ skeletal electrons. Incorporation of an interstitial atom into the center of an isolated hypoelectronic indium polyhedron splits the single multicenter core bond found in an empty globally delocalized polyhedron into two or more core bonds, corresponding to the coordination number and sp^n hybrid orbital orientation of the interstitial atom. Thus, the compound $K_8In_{10}Zn$ can be regarded as a linear two-coordinate Zn^{2+} complex of the bidentate In_{10}^{10-} ligand and the compound $K_{10}In_{10}Ni$ can be regarded as a tetrahedral four-coordinate Ni^0 complex of the tetradentate In_{10}^{10-} ligand. This theory predicts the existence of alkali-metal–indium–coinage metal ternary phases such as K_8In_9Cu , which would correspond to a trigonal Cu^+ complex of a tridentate In_9^{9-} ligand. In such structures, the hypoelectronic anionic indium polyhedron can be regarded as a multidentate ligand encapsulating the interstitial atom.

Keywords: Metal cluster topology; Indium complexes; Cluster complexes

1. Introduction

The importance and stability of the deltahedral borane anions $B_nH_n^{2-}$ ($6 \leq n \leq 12$) [2,3] make of interest the properties of polyhedral clusters of the heavier congeners of boron, namely, aluminum, gallium, indium and thallium ¹. Known aluminum clusters containing isolated deltahedra are limited to the recently discovered [4] icosahedral $iBu_{12}Al_{12}^{2-}$, although the tendency of

aluminum to prefer icosahedral structures undoubtedly relates to the frequent occurrence of aluminum in icosahedral quasicrystal alloys [5–9]. Gallium forms numerous alkali metal compounds with structures containing gallium deltahedra [10–13], but such gallium deltahedra are always linked to the remainder of the structure through *exo*-bonds from essentially all of the gallium vertices. Thus, the polyhedral cluster chemistries of the three lightest icosogens ¹, namely, boron, aluminum and gallium, although each is different from the other, have the common feature of *exo*-bonding from each of the polyhedral vertices either to monovalent groups such as hydrogen, alkyl

[☆] For Part 16 see Ref. [1].

¹ For convenience the group B, Al, Ga, In, Tl (Group 13) elements are called *icosogens* in view of the characteristic occurrence of icosahedral structures in B, Al and Ga clusters.

or halogen, or to another metal atom in an infinite metal subnetwork.

New features emerge in the polyhedral cluster chemistry of the two heaviest icosogens, namely, indium and thallium, since these metals tend to form isolated naked clusters with no *exo*-bonds from any polyhedral vertices. In fact thallium is at the edge of the region of the Periodic Table associated with the chemistry of Zintl anions [14], namely, isolated bare anionic clusters such as TlSn_8^{3-} . However, bare homoatomic icosogen clusters of the type M_n^{z-} ($\text{M} = \text{In, Tl}$) have too few skeletal electrons to form globally delocalized deltahedra with the required $2n + 2$ skeletal electrons without excessively high negative charges, e.g. In_{12}^{14-} for a globally delocalized indium icosahedron. Indium avoids this difficulty by forming new types of hypoelectronic (electron-poor) clusters which require far less than the apparent $2n + 2$ skeletal electrons for globally delocalized deltahedra. These hypoelectronic indium polyhedra, found in various binary and ternary intermetallic phases containing indium and alkali metals as well as sometimes a third metal, are very different from the capped deltahedra found in hypoelectronic metal carbonyl clusters, such as bicapped tetrahedral $\text{Os}_6(\text{CO})_{18}$ and capped octahedral $\text{Rh}_7(\text{CO})_{16}^{3-}$. This paper examines these hypoelectronic indium polyhedra by graph-theory-derived methods described in detail elsewhere [15–18].

2. Background

The atoms at the vertices of a polyhedral cluster can be classified as light atoms or heavy atoms. A light atom such as boron or carbon uses only its *s* and *p* orbitals for chemical bonding and therefore has four valence orbitals (sp^3). A heavy atom such as a transition or post-transition metal, including indium, uses *s*, *p* and *d* orbitals for chemical bonding and, therefore, has nine valence orbitals (sp^3d^5). A normal vertex atom in a polyhedral cluster uses three of its k^2 valence orbitals ($k = 2$ for a light atom and $k = 3$ for a heavy atom) for skeletal bonding; these three orbitals are called internal orbitals. The use of three internal orbitals from a normal bare post-transition-metal vertex atom for the skeletal bonding in a metal cluster leaves six external orbitals for a total of six lone electron pairs, which require 12 external electrons. Thus, a normal indium vertex using three internal orbitals can donate only a single skeletal electron (i.e., 13 valence electrons minus 12 external electrons equals one skeletal electron). This leads to excessively high negative charges on bare homoatomic indium clusters with conventional deltahedral structures requiring $2n + 2$ skeletal electrons such as those found for the borane anions $\text{B}_n\text{H}_n^{2-}$ ($6 \leq n \leq 12$).

The 12 external electrons of a normal bare post-transition-metal vertex in a metal cluster may be divided

into two types, namely, the ten non-bonding *d* electrons and the two electrons of an external lone pair analogous to the B–H bonding pair in the polyhedral boranes $\text{B}_n\text{H}_n^{2-}$ ($6 \leq n \leq 12$). In this way a normal post-transition-metal vertex such as indium may be considered to use a four-orbital sp^3 bonding manifold just like the four-orbital sp^3 bonding manifolds of light vertex atoms such as boron or carbon. This suggests the possibility of a hypervalent post-transition-metal vertex in which one or more of the *d* orbitals participates in the skeletal bonding. Since the valence *d* orbitals of post-transition metals are filled, their involvement in skeletal bonding provides a means for increasing the number of skeletal electrons by one electron pair for the involvement of each *d* orbital. More specifically, a bare hypervalent indium vertex using a five-orbital sp^3d manifold with only four rather than five non-bonding *d* orbitals would be a donor of 13 minus two (the external lone pair) minus eight (the four remaining non-bonding *d* orbitals) equals three skeletal electrons. The participation of *d* orbitals of indium vertices in skeletal bonding in indium clusters is consistent with similar *d* orbital participation in known indium complexes [19] with coordination numbers greater than four, such as InCl_5^{2-} .

A hypervalent indium vertex in a bare cluster uses one of its five bonding orbitals for the external lone pair leaving four rather than the normal three orbitals for skeletal bonding. Hypervalent vertices with $\text{sp}^3\text{d}(x^2 - y^2)$ hybridized orbitals were previously [20] invoked for alkylphosphinidene (RP) vertices in certain metal carbonyl clusters. However, since phosphorus *d* orbitals are originally empty, hypervalent phosphorus vertices contribute the same number of skeletal electrons as normal phosphorus vertices. This contrasts with hypervalent (sp^3d) indium vertices which contribute two more skeletal electrons than normal (sp^3) indium vertices, since the indium *d* orbitals are originally filled. Thus, the use of hypervalent rather than normal indium vertices is a natural way of relieving the apparent electron poverty (hypoelectronicity) in indium cluster polyhedra.

The four valence orbitals on each normal vertex atom in a delocalized polyhedral cluster may be conveniently divided into one external orbital, two equivalent twin internal orbitals and one unique internal orbital. The external orbital is used to form a σ bond to an external group or, in the case of bare post-transition-metal clusters, contains a non-bonding lone pair. The unique internal orbitals, also called radial orbitals [21], form a multicenter core bond in the center of the polyhedron. The twin internal orbitals, also called tangential orbitals [20], form two-center bonds in the surface of the polyhedron. In globally delocalized deltahedra and similar clusters the external and unique internal orbitals form linear $\text{sp}(z)$ hybrid orbitals, whereas the remaining two *p* orbitals are the twin internal orbitals. Similarly,

the five valence orbitals, $sp^3d(x^2-y^2)$ on a hypervalent vertex atom, may be conveniently divided into one external orbital, three equivalent triplet internal orbitals and one unique orbital. Again the external and unique internal orbitals form linear $sp(z)$ hybrid orbitals leaving two p orbitals and the $d(x^2-y^2)$ orbital to form three equivalent hybrid orbitals for the surface bonding. Because of the larger number of surface orbitals generated by hypervalent vertex atoms relative to normal vertex atoms, some of the surface bonds will be three-center rather than two-center bonds without affecting the skeletal electron count.

The globally delocalized deltahedra with n vertices have $2n+2$ skeletal electrons with $2n$ of these electrons arising from the surface bonding and the remaining two electrons occupying the single bonding molecular orbital arising from the multicenter core bond. Hyperelectronic (electron-rich) polyhedra with more than $2n+2$ apparent skeletal electrons have one or more non-triangular faces, which may be regarded topologically as 'holes' in an otherwise closed surface. The electron richness of such hyperelectronic polyhedra arises from splitting the n -center core bond of the $2n+2$ skeletal electron globally delocalized system into a set of two or more bonds, consisting of a multicenter core bond using fewer than n unique internal orbitals and one or more additional multicenter bonds located above each of the 'holes' (i.e., non-triangular faces), thereby resulting in increasing localization of the chemical bonding. Such hyperelectronic polyhedra are found in the *nido* boron hydrides, which have $2n+4$ apparent skeletal electrons. Hypoelectronic (electron-poor) polyhedra with less than $2n+2$ apparent skeletal electrons have structures based on a central deltahedron having one or more capped (triangular) faces. The internal orbitals of the capping vertices in the hypoelectronic polyhedra found in metal carbonyl chemistry, such as various capped octahedra, do not participate in the multicenter core bond but instead are linked to the remainder of the cluster through two-center two-electron bonds to each vertex of the triangular face being capped, thereby leading to one tetrahedral cavity for each capping vertex. If the central deltahedron is an octahedron or other deltahedron without degree-three vertices, then the tetrahedral cavities are regions of edge-localized bonding attached to a globally delocalized central deltahedron.

The process of capping to form hypoelectronic polyhedra with less than $2n+2$ apparent skeletal electrons can be supplemented in extremely electron-poor structures, such as those found in the indium clusters, by another process conveniently called 'flattening' since it consists of flattening the tetrahedral or pyramidal cavity formed by the capping vertex and the vertices of the face being capped. Flattening opens at least some of the edges of the capped face and pushes the capping

vertex closer to the center of the polyhedron. Flattening can bring the unique internal orbital of the capping vertex close enough to the center of the polyhedron to participate in the multicenter core bonding, thereby increasing the delocalization of the system. Flattening of the tetrahedral cavity formed by capping a triangular face is depicted in Fig. 1. The pyramidal cavity formed by capping square or rectangular faces can also be flattened, thus converting, for example, the D_{2d} bicapped square antiprism found in $B_{10}H_{10}^{2-}$ to the ten-vertex polyhedron found in the centered indium cluster $K_8In_{10}Zn$ (Fig. 2). In Figs. 1 and 2 the dashed and hashed lines represent intervertex distances too long to be considered edges.

The flattening of the pyramidal cavities generated by selected capping vertices in hypoelectronic indium polyhedra with 10 and 11 vertices relates to the location of the hypervalent indium vertices. Reasonable electron counts and bonding schemes are obtained if all of the indium vertices at apices of flattened pyramidal cavities are hypervalent and the remaining indium vertices are all normal. The selective location of hypervalent indium atoms at apices of flattened pyramidal cavities may relate to the lower local curvature at such vertices, which is better accommodated by the four internal orbitals (three triplet internal orbitals and one unique internal orbital) of a hypervalent sp^3d indium atom than the three internal orbitals (two twin internal orbitals and one unique internal orbital) of a normal sp^3 indium atom.

Several clusters discussed in this paper contain late transition metals (e.g., nickel, palladium, platinum) or post-transition elements (e.g., zinc) as interstitial atoms located in the center of the indium polyhedron. The five d orbitals of these interstitial atoms are regarded as non-bonding orbitals and thus contain ten non-bonding electrons. For this reason an interstitial nickel, palladium or platinum atom is a donor of zero skeletal electrons, an interstitial copper, silver or gold atom is

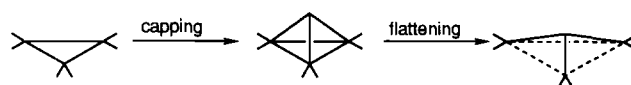


Fig. 1. Capping a triangular face followed by flattening the resulting tetrahedral cavity.

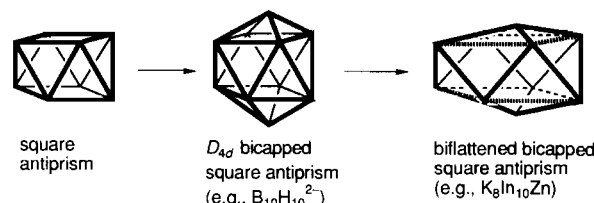


Fig. 2. Capping of a square antiprism to give a D_{4d} bicapped square antiprism followed by flattening the two caps to give the ten-vertex polyhedron found in $K_8In_{10}Zn$. Dashed and hashed lines indicate the position of edges broken during the flattening process.

a donor of a single skeletal electron, and an interstitial zinc, cadmium or mercury atom is a donor of two skeletal electrons. This electron-counting scheme relates to the fact that the interstitial nickel atom in $\text{Ni}_{13}\text{Sb}_2(\text{CO})_{24}^{4-}$ is also a donor of zero skeletal electrons [22,23]. Furthermore, the non-bonding role of the d electrons in such interstitial atoms means that only their s and p orbitals overlap with the unique internal orbitals (radial orbitals) of the vertices of the surrounding indium polyhedron. A result of the interstitial late transition or post-transition-metal atoms in centered indium clusters is the splitting of the multicenter core bond into several multicenter bonds oriented around the interstitial atom in accord with a reasonable sp^n hybridization scheme, e.g. linear sp for zinc, tetrahedral sp^3 for nickel, palladium, platinum, etc. In this sense the hypoelectronic anionic indium polyhedron can be regarded as a multidentate ligand encapsulating the interstitial atom. Such an interpretation appears to be fully consistent with the observed electron counts in the centered hypoelectronic indium clusters which have so far been characterized.

3. Binary alkali-metal–indium intermetallics: empty indium clusters

The first alkali-metal–indium intermetallic to be prepared containing an indium cluster polyhedron was K_8In_{11} reported by Sevov and Corbett in 1991 [24]. This cluster contains the characteristic idealized D_{3h} triflattened pentacapped trigonal prism in which only the three pyramidal cavities formed by capping the rectangular faces of the trigonal prism are flattened and the remaining two tetrahedral cavities formed by capping the triangular faces of the trigonal prism remain unflattened (Fig. 3). Extended Hückel calculations [23,25] on K_8In_{11} suggest that the closed-shell configuration for this cluster is In_{11}^{7-} , in accord with the observed metallic behavior of K_8In_{11} arising from delocalization of the extra electron. More convincing evidence that In_{11}^{7-} is a closed-shell electronic con-

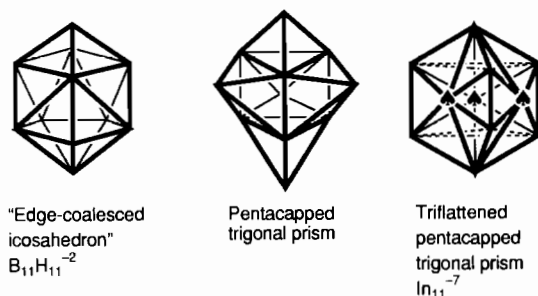


Fig. 3. Chemically significant 11-vertex deltahedra. In the triflattened pentacapped trigonal prism the apices of the flattened pyramidal cavities are indicated by spades (♠) and the locations of the edges broken during flattening are indicated by dashed lines.

figuration for this type of cluster came from the subsequent discovery [26] of $\text{K}_8\text{In}_{10}\text{Hg}$, also shown to have a triflattened pentacapped trigonal prismatic structure but found to be diamagnetic in accord with a closed-shell electronic configuration for $\text{In}_{10}\text{Hg}^{8-}$ isoelectronic with In_{11}^{7-} . The relationship of the triflattened pentacapped trigonal prism of In_{11}^{7-} to that of other 11-vertex cluster structures is depicted in Fig. 3. Note that the triflattened pentacapped trigonal prism is related to the unflattened pentacapped trigonal prism by a sextuple diamond–square–diamond process [27–29], since six new edges are added after flattening to replace the six edges broken during flattening.

The triflattened pentacapped trigonal prism in In_{11}^{7-} can be considered to have three hypervalent and eight normal indium vertices in accord with the three flattened pyramidal cavities. The number of skeletal electrons in In_{11}^{7-} corresponds to the 24 electrons required for an 11-vertex deltahedron ($24 = 2n + 2$ for $n = 11$) by the following electron counting scheme:

8 normal In vertices: $8 \times 1 =$	8 skeletal electrons
3 hypervalent In vertices: $3 \times 3 =$	9 skeletal electrons
-7 charge =	7 skeletal electrons
<hr/>	
Total skeletal electrons =	24 skeletal electrons

4. Centered indium clusters

There are two known types of centered indium clusters in ternary intermetallic phases containing indium, potassium and a third metal (Fig. 4), namely, biflattened bicapped square antiprismatic $\text{K}_8\text{In}_{10}\text{Zn}$ [30] and tetraflattened tetracapped trigonal prismatic $\text{K}_{10}\text{In}_{10}\text{M}$ ($\text{M} = \text{Ni}, \text{Pd}, \text{Pt}$) [31]. Triflattened tricapped trigonal prismatic centered indium clusters can be predicted to occur in ternary alkali-metal–indium–coinage metal phases such as $\text{K}_8\text{In}_9\text{Cu}$ (Fig. 4) but these have not yet been found. The electron counting in these centered indium clusters is outlined below.

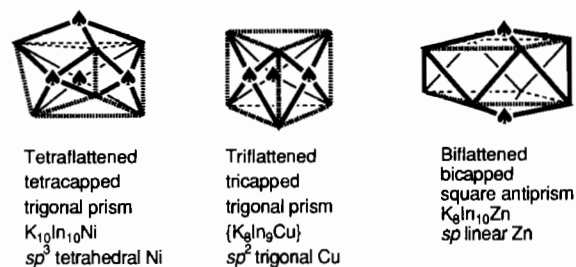


Fig. 4. Hypoelectronic polyhedra found in the centered indium clusters $\text{K}_{10}\text{In}_{10}\text{M}$ ($\text{M} = \text{Ni}, \text{Pd}, \text{Pt}$) and $\text{K}_8\text{In}_{10}\text{Zn}$, as well as that predicted for $\text{K}_8\text{In}_9\text{M}'$ ($\text{M}' = \text{Cu}, \text{Ag}, \text{Au}$). Vertices of flattened pyramidal cavities are indicated by spades (♠).

4.1. $K_8In_{10}Zn$

The biflattened bicapped square antiprism in $K_8In_{10}Zn$ (Fig. 4) [29] requires two hypervalent and eight normal indium vertices leading to the following electron counting scheme:

8 normal In vertices: $8 \times 1 =$	8 skeletal electrons
2 hypervalent In vertices: $2 \times 3 =$	6 skeletal electrons
1 interstitial Zn atom: $12 - 10 =$	2 skeletal electrons
-8 charge =	8 skeletal electrons
Total skeletal electrons	24 skeletal electrons

These 24 skeletal electrons can be distributed as follows:

10 surface bonds: $10 \times 2 =$	20 skeletal electrons
2 core bonds: $2 \times 2 =$	4 skeletal electrons
Total skeletal electrons required	24 skeletal electrons

The two core bonds can correspond to sp linear hybrids of the central zinc atom overlapping with the unique internal orbitals of each hypervalent indium atom supplemented by additional overlap with the unique internal orbitals from the other indium vertices. This interpretation of the bonding in $In_{10}Zn^{8-}$ is equivalent to regarding this cluster as two In_5Zn octahedra sharing the zinc vertex with a six-center core bond in the center of each octahedral cavity. Alternatively, the biflattened bicapped square antiprismatic In_{10} cluster can be regarded as a cryptand with a preference for encapsulating linear two-coordinate atoms such as zinc. In this interpretation the $In_{10}Zn^{8-}$ anion can be regarded as a linear Zn^{2+} complex of the bidentate cryptate In_{10}^{10-} anion. However, the heavier congener of zinc, namely, mercury, appears to be too large to be encapsulated in this manner, since the cluster $In_{10}Hg^{8-}$ has a different structure in which the mercury is a surface atom like the ten indium atoms, leading to the triflattened pentacapped trigonal prismatic structure discussed above (Fig. 3) [24].

4.2. $K_{10}In_{10}M$ ($M = Ni, Pd, Pt$)

The tetraflattened tetracapped trigonal prism in $K_{10}In_{10}M$ ($M = Ni, Pd, Pt$) [30] requires four hypervalent and six normal indium vertices leading to the following electron counting scheme:

6 normal In vertices: $6 \times 1 =$	6 skeletal electrons
4 hypervalent In vertices: $4 \times 3 =$	12 skeletal electrons
Interstitial M atom ($M = Ni, Pd, Pt$):	
$10 - 10 =$	0 skeletal electrons
-10 charge =	10 skeletal electrons
Total skeletal electrons	28 skeletal electrons

These 28 skeletal electrons can be distributed as follows:

10 surface bonds: $10 \times 2 =$	20 skeletal electrons
4 core bonds: $4 \times 2 =$	8 skeletal electrons
Total skeletal electrons required	28 skeletal electrons

The four core bonds can correspond to sp^3 tetrahedral hybrids of the central M atom overlapping with the unique internal orbitals of the four hypervalent indium atoms in roughly tetrahedral positions (Fig. 4), with additional overlap with the unique internal orbitals from the other indium vertices. The tetrahedral coordination of the nickel atom in $K_{10}In_{10}Ni$ may be regarded as analogous to the tetrahedral coordination of nickel in $Ni(CO)_4$. In this interpretation the $In_{10}Ni^{10-}$ anion can be regarded as a tetrahedral $Ni(0)$ complex of the tetradentate In_{10}^{10-} cryptate-like anion.

4.3. K_8In_9M' ($M' = Cu, Ag, Au$)

Coinage metals, especially copper, are predicted to occur as interstitial atoms in alkali-metal-indium-coinage metal ternary phases with triflattened tricapped trigonal prismatic K_8In_9M' ($M' = Cu, Ag, Au$) with a trigonally coordinated interstitial coinage metal atom appearing to be particularly favorable (Fig. 4) using the following electron-counting scheme for K_8In_9Cu :

6 normal In vertices: $6 \times 1 =$	6 skeletal electrons
3 hypervalent In vertices: $3 \times 3 =$	9 skeletal electrons
Interstitial M atom ($M = Cu, Ag, Au$):	
$11 - 10 =$	1 skeletal electron
-8 charge =	8 skeletal electrons
Total skeletal electrons	24 skeletal electrons

These 24 skeletal electrons can be distributed as follows:

9 surface bonds: $9 \times 2 =$	18 skeletal electrons
3 core bonds: $3 \times 2 =$	6 skeletal electrons
Total skeletal electrons required	24 skeletal electrons

The three core bonds may correspond to sp^2 trigonal hybrids of the central copper atom overlapping with the unique internal orbitals of the three hypervalent indium atoms in trigonal positions (Fig. 4) of the triflattened tricapped trigonal prism, with additional overlap with the unique internal orbitals from the other indium vertices, leading to three four-center $CuIn_3$ bonds trigonally oriented around the interstitial copper atom.

5. Conclusions

Analyses of the structures and electron counts for the known isolated indium clusters found in binary and ternary alkali-metal-indium phases suggest the involvement of filled indium d orbitals in the skeletal bonding to relieve the apparent electron poverty in the hypoelectronic indium cluster polyhedra. The unusual shapes of the hypoelectronic polyhedra are based on capping a triangular or rectangular face of a smaller polyhedron,

followed by flattening the resulting pyramidal cavity so that the capping vertex at the pyramid apex moves closer to the center of the central polyhedron. Reasonable electron counts and globally delocalized bonding schemes for the hypoelectronic indium clusters are then obtained if all of the indium apices of the flattened pyramidal cavities are hypervalent using sp^3d five-orbital manifolds and the remaining indium vertices are normal using sp^3 four-orbital manifolds, like typical vertex atoms in boranes, carboranes and post-transition-metal 'Zintl-type' clusters. Incorporation of an interstitial atom into the center of an isolated hypoelectronic indium polyhedron splits the single multicenter core bond found in an empty globally delocalized polyhedron into two or more core bonds corresponding to the coordination number and orientation of the interstitial atom. Thus, the compound $K_8In_{10}Zn$ can be regarded as a linear two-coordinate Zn^{2+} complex of the bidentate In_{10}^{10-} ligand and the compound $K_{10}In_{10}Ni$ can be regarded as a tetrahedral four-coordinate Ni^0 complex of the tetradentate In_{10}^{10-} ligand. This theory predicts the existence of alkali-metal-indium-coinage metal clusters such as K_8In_9Cu , which may be regarded as a trigonal Cu^+ complex of a tridentate In_9^{9-} ligand. In such structures the hypoelectronic anionic indium polyhedron can be regarded as a multidentate cryptate-like ligand encapsulating the interstitial atom.

References

- [1] R.B. King, *Inorg. Chim. Acta*, 227 (1994) 207.
- [2] E.L. Muetterties and W.H. Knoth, *Polyhedral Boranes*, Marcel Dekker, New York, 1968.
- [3] E.L. Muetterties (ed.), *Boron Hydride Chemistry*, Academic Press, New York, 1975.
- [4] W. Hiller, K.-W. Klinkhammer, W. Uhl and J. Wagner, *Angew. Chem., Int. Ed. Engl.*, 30 (1991) 179.
- [5] D. Levine and P.J. Steinhardt, *Phys. Rev. Lett.*, 53 (1984) 2477.
- [6] D. Levine and P.J. Steinhardt, *Phys. Rev.*, 34 (1986) 596.
- [7] M. Audier, C. Janot, M. de Boissieu and B. Dubost, *Philos. Mag. B*, 60 (1989) 437.
- [8] R.B. King, *Inorg. Chim. Acta*, 181 (1991) 217.
- [9] C. Janot, *Quasicrystals: A Primer*, Clarendon, Oxford, 1992.
- [10] C. Belin and R.G. Ling, *J. Solid State Chem.*, 48 (1983) 40.
- [11] C. Belin and M. Tillard-Charbonnel, *Prog. Solid State Chem.*, 22 (1993) 59.
- [12] R.B. King, *Inorg. Chem.*, 28 (1989) 2796.
- [13] J.K. Burdett and E. Canadell, *J. Am. Chem. Soc.*, 112 (1990) 7207.
- [14] J.D. Corbett, *Chem. Rev.*, 85 (1985) 383.
- [15] R.B. King and D.H. Rouvray, *J. Am. Chem. Soc.*, 99 (1977) 7834.
- [16] R.B. King, *J. Math. Chem.*, 1 (1987) 249.
- [17] R.B. King, *J. Phys. Chem.*, 92 (1988) 4452.
- [18] R.B. King, *Applications of Graph Theory and Topology in Inorganic Cluster and Coordination Chemistry*, CRC, Boca Raton, FL, 1993.
- [19] A.J. Carty and D.J. Tuck, *Prog. Inorg. Chem.*, 19 (1975) 243.
- [20] R.B. King, *New J. Chem.*, 13 (1989) 293.
- [21] K. Wade, *Adv. Inorg. Chem. Radiochem.*, 18 (1976) 1.
- [22] V.G. Albano, F. Demartin, M.C. Iapalucci, B. Longoni, A. Sironi and V. Zanotti, *Chem. Commun.*, (1990) 547.
- [23] R.B. King, *Rev. Roum. Chim.*, 36 (1991) 379.
- [24] S.C. Sevov and J.D. Corbett, *Inorg. Chem.*, 30 (1991) 4875.
- [25] W. Blase, G. Cordier, V. Müller, U. Häußermann, R. Nesper and M. Somer, *Z. Naturforsch., Teil B*, 48 (1993) 754.
- [26] S.C. Sevov, J.E. Ostenson and J.D. Corbett, *J. Alloys Compounds*, 202 (1993) 289.
- [27] W.N. Lipscomb, *Science*, 153 (1966) 373.
- [28] R.B. King, *Inorg. Chim. Acta*, 49 (1981) 237.
- [29] R.B. King, *J. Math. Chem.*, 12 (1993) 9.
- [30] S.C. Sevov and J.D. Corbett, *Inorg. Chem.*, 32 (1993) 1059.
- [31] S.C. Sevov and J.D. Corbett, *J. Am. Chem. Soc.*, 115 (1993) 9089.